

# A Newcastle disease virus-vector expressing a prefusion-stabilized spike protein of SARS-CoV-2 induces protective immune responses against prototype virus and variants of concern in mice and hamsters

**Weina Sun**

Icahn School of Medicine at Mount Sinai <https://orcid.org/0000-0002-2435-5047>

**Yonghong Liu**

Icahn School of Medicine at Mount Sinai

**Fatima Amanat**

Icahn School of Medicine at Mount Sinai <https://orcid.org/0000-0002-8029-8227>

**Irene González-Domínguez**

Icahn School of Medicine at Mount Sinai

**Stephen McCroskey**

Icahn School of Medicine at Mount Sinai

**Stefan Slamanig**

Icahn School of Medicine at Mount Sinai

**Lynda Coughlan**

University of Maryland School of Medicine <https://orcid.org/0000-0001-9880-6560>

**Victoria Rosado**

Icahn School of Medicine at Mount Sinai

**Nicholas Lemus**

Icahn School of Medicine at Mount Sinai

**Sonia Jangra**

Icahn School of Medicine at Mount Sinai

**Raveen Rathnasinghe**

Icahn School of Medicine at Mount Sinai

**Michael Schotsaert**

Icahn School of Medicine at Mount Sinai <https://orcid.org/0000-0003-3156-3132>

**Jose Martinez**

Icahn School of Medicine at Mount Sinai

**Kaori Sano**

Icahn School of Medicine at Mount Sinai

**Ignacio Mena**

Icahn School of Medicine at Mount Sinai <https://orcid.org/0000-0001-5464-7086>

**Bruce Innis**

PATH <https://orcid.org/0000-0002-1753-7248>

**Ponthip Wirachwong**

The Government Pharmaceutical Organization

**Duong Huu Thai**

Institute of Vaccines and Medical Biologicals

**Ricardo Oliveira**

Instituto Butantan

**Rami Scharf**

PATH

**Richard Hjorth**

PATH

**Rama Raghunandan**

PATH

**Florian Krammer**

Icahn School of Medicine at Mount Sinai <https://orcid.org/0000-0003-4121-776X>

**Adolfo Garcia-Sastre**

Icahn School of Medicine at Mount Sinai <https://orcid.org/0000-0002-6551-1827>

**Peter Palese (✉ [peter.palese@mssm.edu](mailto:peter.palese@mssm.edu))**

Mount Sinai School of Medicine <https://orcid.org/0000-0002-0337-5823>

---

**Article**

**Keywords:** SARS-CoV-2, COVID-19 vaccine, Newcastle disease virus

**Posted Date:** July 1st, 2021

**DOI:** <https://doi.org/10.21203/rs.3.rs-676469/v1>

**License:**  This work is licensed under a Creative Commons Attribution 4.0 International License.

[Read Full License](#)

---

**Version of Record:** A version of this preprint was published at Nature Communications on October 27th, 2021. See the published version at <https://doi.org/10.1038/s41467-021-26499-y>.

1 **A Newcastle disease virus-vector expressing a prefusion-stabilized spike protein of SARS-CoV-2**  
2 **induces protective immune responses against prototype virus and variants of concern in mice and**  
3 **hamsters**

4  
5 Weina Sun<sup>1</sup>, Yonghong Liu<sup>1</sup>, Fatima Amanat<sup>1,2</sup>, Irene González-Domínguez<sup>1</sup>, Stephen McCroskery<sup>1,3</sup>,  
6 Stefan Slamanig<sup>1</sup>, Lynda Coughlan<sup>6,12</sup>, Victoria Rosado<sup>1</sup>, Nicholas Lemus<sup>1</sup>, Sonia Jangra<sup>1,4</sup>, Raveen  
7 Rathnasinghe<sup>1,2,4</sup>, Michael Schotsaert<sup>1,4</sup>, Jose Martinez<sup>1</sup>, Kaori Sano<sup>1</sup>, Ignacio Mena<sup>1,4</sup>, Bruce L Innis<sup>10</sup>,  
8 Ponthip Wirachwong<sup>8</sup>, Duong Huu Thai<sup>7</sup>, Ricardo Das Neves Oliveira<sup>9</sup>, Rami Scharf<sup>10</sup>, Richard Hjorth<sup>10</sup>,  
9 Rama Raghunandan<sup>10</sup>, Florian Krammer<sup>1,11</sup>, Adolfo García-Sastre<sup>1,3,4,5,11</sup> and Peter Palese<sup>1,3\*</sup>

10  
11 <sup>1</sup> Department of Microbiology, Icahn School of Medicine at Mount Sinai, New York, NY 10029, USA

12 <sup>2</sup> Graduate School of Biomedical Sciences, Icahn School of Medicine at Mount Sinai, New York, NY  
13 10029, USA

14 <sup>3</sup> Department of Medicine, Icahn School of Medicine at Mount Sinai, New York, NY 10029, USA

15 <sup>4</sup> Global Health Emerging Pathogens Institute, Icahn School of Medicine at Mount Sinai, New York, NY  
16 10029, USA

17 <sup>5</sup> The Tisch Cancer Institute, Icahn School of Medicine at Mount Sinai, New York, NY 10029, USA

18 <sup>6</sup> University of Maryland School of Medicine, Department of Microbiology and Immunology,  
19 Baltimore, MD 21201, USA

20 <sup>7</sup> Institute of Vaccines and Medical Biologicals, Nha Trang City, Khanh Hoa Province, Vietnam

21 <sup>8</sup> The Government Pharmaceutical Organization, Bangkok 10400, Thailand

22 <sup>9</sup> Instituto Butantan, São Paulo, SP, 05503-900, Brazil

23 <sup>10</sup> PATH, Center for Vaccine Access and Innovation, Washington, DC 20001, USA

24 <sup>11</sup> Department of Pathology, Icahn School of Medicine at Mount Sinai, New York, NY 10029, USA

25 <sup>12</sup> University of Maryland School of Medicine, Center for Vaccine Development and Global Health  
26 (CVD), Baltimore, MD 21201, USA

27  
28 \* To whom correspondence should be addressed: peter.palese@mssm.edu  
29

30 **Abstract**

31 Rapid development of coronavirus disease 2019 (COVID-19) vaccines and expedited authorization  
32 for use and approval has been proven beneficial to mitigate severe acute respiratory syndrome coronavirus  
33 2 (SARS-CoV-2) spread and given hope in this desperate situation. It is believed that sufficient supplies  
34 and equitable allocations of vaccines are necessary to limit the global impact of the COVID-19 pandemic

35 and the emergence of additional variants of concern. We have developed a COVID-19 vaccine based on  
36 Newcastle disease virus (NDV) that can be manufactured at high yields in embryonated eggs. Here we  
37 provide evidence that the NDV vector expressing an optimized spike antigen (NDV-HXP-S), upgraded  
38 from our previous construct, is a versatile vaccine that can be used live or inactivated to induce strong  
39 antibody responses and to also cross-neutralize variants of concern. The immunity conferred by NDV-HXP-  
40 S effectively counteracts SARS-CoV-2 infection in mice and hamsters. It is noteworthy that vaccine lots  
41 produced by existing egg-based influenza virus vaccine manufacturers in Vietnam, Thailand and Brazil  
42 exhibited excellent immunogenicity and efficacy in hamsters, demonstrating that NDV-HXP-S vaccines  
43 can be quickly produced at large-scale to meet global demands.

44  
45

## 46 **Introduction**

47 The coronavirus disease 2019 (COVID-19) pandemic caused by severe acute respiratory syndrome  
48 coronavirus 2 (SARS-CoV-2) has brought disastrous outcomes to public health, education and economics  
49 worldwide. Emerged variants of concern that are currently circulating could threaten the prior preventive  
50 achievements if not managed properly. The rollout of COVID-19 vaccines such as mRNA vaccines (Pfizer  
51 and Moderna), inactivated virus vaccines (Sinovac, Sinopharm), adenovirus-vector vaccines (AstraZeneca,  
52 CanSino Biologics, Gamaleya Research Institute and J&J) have helped to contain the spread of the virus  
53 tremendously, stressing the importance of prophylactic measures. However, despite the high efficacy of  
54 mRNA vaccines, availability of such vaccines to developing countries is restricted due to cold or ultra-cold  
55 chain requirements and lack of manufacturing infrastructure and capacity. Indeed, with North America and  
56 Europe having the highest vaccination rates, vaccine resources are much less accessible to developing  
57 countries in Latin America, Asia and Africa (1) . Such inequitable availability of vaccine delays prompt  
58 control of COVID-19 and increases the risk of additional variants to emerge. This highlights the urgent  
59 need for affordable vaccines that can be produced locally.

60 We have previously developed a Newcastle disease virus (NDV)-based COVID-19 vaccine, in  
61 which a membrane-anchored spike protein is expressed on the surface of the NDV virion. This NDV-vector  
62 could be used either as a live vaccine or an inactivated vaccine (2, 3). Here we describe a next-generation  
63 version of the NDV vector expressing a prefusion spike protein stabilized by HexaPro (HXP) mutations,  
64 which are reported to contribute to high protein yield, favorable conformation and enhanced stability (4).  
65 This construct is designated NDV-HXP-S. As an egg-based vaccine like the influenza virus vaccine, NDV-  
66 HXP-S is suitable for large-scale production to cover a fair share of global demands. A survey conducted  
67 by The World Health Organization (WHO) estimated the production capacity for pandemic influenza  
68 vaccines (monovalent) could reach ~4.15 billion doses in 12 months by 31 established manufacturers

69 worldwide, among which 28 manufacturers have egg-based facility producing 79% of total doses (5). This  
70 report realistically reflects the feasibility of manufacturing large quantify of NDV-based COVID-19  
71 vaccine, since few modifications to the influenza virus vaccine manufacturing process are needed.  
72 Moreover, this estimation assumes the dose of NDV-based vaccine required will match that of monovalent  
73 pandemic influenza vaccines (15 µg/0.5mL), without adjusting for the potential antigen-sparing effect of  
74 adjuvants (5). A safe and inexpensive adjuvant could likely expand the number of the doses per egg.

75 In the belief that NDV-HXP-S could be the solution for self-sufficient supplies of COVID-19  
76 vaccine in many low- and middle-income countries (LMICs), in this study we thoroughly evaluated the  
77 immunogenicity and protective efficacy of live and inactivated NDV-HXP-S in preclinical mouse and  
78 Golden Syrian hamster models. We assessed the beta-propiolactone (BPL)-inactivated NDV-HXP-S  
79 whole-virion vaccine (GMP manufactured in Thailand, Vietnam and Brazil) via the intramuscular (IM)  
80 route using a two-dose regimen. In addition, we explored the possibility of using the NDV-HXP-S as a live  
81 vaccine either via the intranasal (IN) route or a combination of IN and IM routes. These preclinical studies  
82 showed that the NDV-HXP-S vaccine in its live or inactivated format was highly immunogenic, inducing  
83 potent binding and neutralizing antibodies (NAbs), which offered protections against SARS-CoV-2  
84 replication or SARS-CoV-2 induced disease *in vivo*. The high levels of NAbs induced by NDV-HXP-S  
85 allowed the variants of concern/interest (B.1.1.7, B.1.351 or P.1) to be neutralized, despite the fact that a  
86 reduction of neutralization titer was observed against the B.1.351 variant. A similar level of reduction has  
87 been shown in other vaccine cohorts as well (6-9). Importantly, Good Manufacturing Practice (GMP)-grade  
88 NDV-HXP-S vaccine lots produced by manufacturers from Vietnam (Institute of Vaccines and Medical  
89 Biologicals, IVAC), Thailand (Government Pharmaceutical Organization, GPO) and Brazil (Instituto  
90 Butantan) showed excellent immunogenicity and protective efficacy in the hamster model, demonstrating  
91 the consistency of the manufacturing process in different locations and the possibility of mass production.  
92 Vaccine trials with the inactivated vaccines have been started in Thailand (NCT04764422, HXP-GPOVac)  
93 and Vietnam (NCT04830800, COVIVAC) and the live vaccine is currently in clinical development in  
94 Mexico (NCT04871737, Patria).

95  
96

## 97 **Results**

### 98 **NDV expressing a membrane-bound pre-fusion stabilized spike protein**

99 To ensure high immunogenicity of the spike antigen expressed by the NDV vector, we improved  
100 the spike construct by introducing the pre-fusion stabilizing HexaPro (HXP) mutations that were identified  
101 and characterized in an earlier study (4). Specifically, we added the HXP mutations into our previously  
102 described S-F chimera (HXP-S), in which the polybasic cleavage site was removed and the transmembrane

103 domain and cytoplasmic tail of the spike were replaced with those from the fusion (F) protein of NDV. The  
104 nucleotide sequence of the construct was codon-optimized for mammalian host expression. The HXP-S  
105 sequence was inserted between the P and M genes of the NDV genome and the virus was rescued (**Fig.**  
106 **1A**). We concentrated the virus in the allantoic fluid through a sucrose cushion and performed a sodium  
107 dodecyl-sulfate polyacrylamide gel electrophoresis (SDS-PAGE) to visualize NDV viral proteins as well  
108 as the presence of the spike protein by Coomassie Blue staining. Compared to the WT NDV, the NDV-  
109 HXP-S showed an extra band between 160 kD and 260 kD below the L protein of the NDV that corresponds  
110 to the size of the uncleaved S0 (**Fig. 1B**).

111

### 112 **Vaccination with inactivated NDV-HXP-S via the intramuscular route induces protective immune** 113 **responses in mice and hamsters**

114 To evaluate the immunogenicity and protective efficacy of the inactivated NDV-HXP-S, we first  
115 performed a dose-ranging study in mice that were “sensitized” by intranasal (IN) administration of a non-  
116 replicating human adenovirus 5 expressing human angiotensin converting enzyme 2 (Ad5-hACE2). Mice  
117 are not naturally susceptible to SARS-CoV-2 infection, but gene delivery of hACE2 to the lungs of mice  
118 using a viral vector such as Ad5-hACE2, can sensitize mice to subsequent infection with SARS-CoV-2  
119 (10).

120 BPL-inactivated NDV-HXP-S with or without an adjuvant CpG 1018 (11) was tested in the study.  
121 Specifically, we immunized BALB/c mice with low doses of NDV-HXP-S at a total protein content of 1  
122  $\mu\text{g}$ , 0.3  $\mu\text{g}$ , 0.1  $\mu\text{g}$ , 0.03  $\mu\text{g}$  and 0.01  $\mu\text{g}$  per mouse without the adjuvant. In the adjuvanted groups, mice  
123 were vaccinated with either 0.1  $\mu\text{g}$  or 0.03  $\mu\text{g}$  of the vaccine in combination with 10  $\mu\text{g}$  or 30  $\mu\text{g}$  of CpG  
124 1018 per mouse. Mice that were immunized with 1  $\mu\text{g}$  of the inactivated WT NDV (vector-only) were used  
125 as negative controls. The inactivated vaccine was administered via the intramuscular route following a  
126 prime-boost regimen at a 3-week interval (**Fig. 2A**). Mice were bled to measure spike-specific serum IgG.  
127 The prime immunization showed a dose-dependent antibody response, in which the adjuvanted groups  
128 appeared to develop higher antibody responses than those which received the same amount of vaccine  
129 without the adjuvant. The antibody titers were greatly enhanced after the boost in all the animals that were  
130 vaccinated with NDV-HXP-S, resulting in no significant differences among the groups (with a marginal  
131 dose-dependent trend). Of note, mice that were vaccinated with as low as 0.03  $\mu\text{g}$  and 0.01  $\mu\text{g}$  of vaccine  
132 per animal also developed good IgG titers, suggesting the vaccine is highly immunogenic (**Fig. 2B**). Further  
133 evaluation of IgG2a over IgG1 ratio in post-boost sera from 3 selected groups, group 1 (1  $\mu\text{g}$ ) representing  
134 animals that received the non-adjuvanted vaccine, group 7 (0.1  $\mu\text{g}$  + 30  $\mu\text{g}$  CpG 1018) representing animals  
135 that received the adjuvanted vaccine and group 10 (WT NDV) as the negative controls, suggested a  $T_H1$ -  
136 biased immune response (12). The CpG 1018 appeared to reinforce a  $T_H1$ -biased immune response, given

137 that a more pronounced difference between the IgG2a and IgG1 levels was observed in the adjuvanted  
138 group as compared to that in the non-adjuvanted group (**Fig. S1A**). To examine the neutralizing activity of  
139 the immune sera from mice, pooled sera from group 1, 7 and 10 were tested. Neutralization titers against  
140 the prototype (WT) USA-WA1/2020 virus as well as two SARS-CoV-2 variants, B.1.1.7 and B.1.351 were  
141 measured (**Fig. 2C**). We observed potent neutralizing activity of mouse sera to the WT strain from group 1  
142 ( $ID_{50} = 669$ ) and group 7 ( $ID_{50} = 627$ ). As expected, mouse sera from both groups neutralized the B.1.1.7  
143 variant equally well (group 1  $ID_{50} = 652$ ; group 7  $ID_{50} = 914$ ). An approximately five-fold reduction of  
144 neutralization titers was observed toward the B.1.351 variant (group 1  $ID_{50} = 132$ ; group 7  $ID_{50} = 132$ ). Our  
145 result is in agreement with decreased neutralization titers of mRNA vaccines that have been reported (6-9),  
146 as the E484K mutation in the B.1.351 variant is mainly responsible for the resistance to NAbs (13, 14). To  
147 assess protection conferred by vaccination, mice were treated with Ad5-hACE2 (10). Five days after the  
148 Ad5-hACE2 treatment, mice were challenged with  $10^5$  plaque forming unit (PFU) of USA-WA1/2020  
149 SARS-CoV-2. Infectious viral titers in the lungs of challenged animals at day 2 and day 5 post-challenge  
150 were measured as the readout of protection. We observed a significant drop of the viral titer in the lung  
151 homogenates of all vaccinated animals compared to those from the negative control group, also in a dose-  
152 dependent manner. At day 5 post-infection, infectious viruses were cleared in all NDV-HXP-S vaccinated  
153 animals (**Fig. 2D**). These results support the conclusion that the inactivated NDV-HXP-S induced strongly  
154 protective antibody responses directed to the spike protein of SARS-CoV-2, with CpG 1018 as a possible  
155 dose-sparing adjuvant.

156 In the hamster model, we evaluated two-doses of inactivated NDV-HXP-S without adjuvants, with  
157 CpG 1018 or AddaVax as the adjuvant. Each hamster was vaccinated intramuscularly with a total of 5  $\mu$ g  
158 of NDV-HXP-S. The negative control group was vaccinated with 5  $\mu$ g of inactivated WT NDV. The  
159 healthy control group was kept unvaccinated. After two doses with a 3-week interval, hamsters were  
160 challenged with  $10^4$  PFU of the USA-WA1/2020 strain, except that the healthy control group was mock-  
161 challenged (**Fig 3A**). Change of body weight, viral titers in the lung homogenates and nasal washes at day  
162 2 and day 5 post-challenge were measured to evaluate protection. In addition, spike-specific IgG titers in  
163 the post-prime and post-boost sera, as well as neutralizing activity in the post-boost sera were measured by  
164 enzyme-linked immunosorbent assay (ELISA) and micro-neutralization assay, respectively. NDV-HXP-S  
165 was found to be highly immunogenic in hamsters as well, with both CpG 1018 and AddaVax increasing  
166 serum IgG (**Fig 3B**). Without any adjuvant, NDV-HXP-S vaccinated hamsters developed potent NAbs in  
167 the post-boost sera ( $ID_{50} = 2429$ ) to the prototype (WT) SARS-CoV-2. AddaVax enhanced NAb titers ( $ID_{50}$   
168 = 3913), but the CpG 1018 did not ( $ID_{50} = 970$ ). Interestingly, the antibodies in the CpG 1018 group  
169 appeared to be more cross-neutralizing to B.1.351 with only a 2-fold decrease ( $ID_{50} = 480$ ). A ~6-fold  
170 reduction of neutralizing titer to the B.1.351 ( $ID_{50} = 425$ ) was observed in the unadjuvanted group, while a

171 ~4-fold reduction of neutralizing activity to the B.1.351 ( $ID_{50}=1144$ ) was observed in the AddaVax group  
172 (**Fig 3C**). After challenge, animals in both adjuvanted groups showed quicker recovery of the body weight  
173 than animals in the unadjuvanted group (**Fig 3D**). Viruses were cleared in the lungs of all NDV-HXP-S  
174 vaccinated hamsters at day 2 except for one out of four animals in the unadjuvanted and CpG 1018 group  
175 which showed low titers that were very close to the limit of detection. Viral load became undetectable at  
176 day 5 post-challenge in all NDV-HXP-S vaccinated hamsters. In addition, all NDV-HXP-S vaccinated  
177 groups showed a reduction of viral titers in the nasal washes compared to control animals (**Fig 3E**). In  
178 conclusion, the inactivated NDV-HXP-S induced high levels of binding and neutralizing antibody  
179 responses in hamsters, significantly reduced viral titers in the lungs and lowered virus shedding from the  
180 nasal cavity. Both CpG 1018 and AddaVax exhibited beneficial adjuvant effects.

181

### 182 **Formulations of inactivated NDV-HXP-S GMP-produced by GPO, IVAC and Instituto Butantan** 183 **are effective in a preclinical hamster study**

184 In the belief that the existing influenza virus vaccine manufacturers should be equipped to produce  
185 NDV-HXP-S, we put this possibility to the test. In collaboration with three influenza virus vaccine  
186 manufacturers (IVAC, GPO, Instituto Butantan) from Vietnam, Thailand and Brazil, pilot GMP lots of  
187 whole BPL- inactivated NDV-HXP-S vaccines were produced. We obtained these vaccine preparations and  
188 subsequently evaluated them in hamsters. Vaccines containing 1  $\mu\text{g}$  of S antigen were administered  
189 intramuscularly to each hamster with or without 100  $\mu\text{g}$  CpG 1018 as the adjuvant following a prime-boost  
190 regimen with a 3-week interval. A PBS-vaccinated negative control and a healthy control group were  
191 included. Two weeks after the boost, animals were challenged with  $10^4$  PFU of the USA-WA1/2020 strain  
192 (**Fig. 4A**). Animals having received vaccines from different producers developed comparable binding IgG  
193 titers, while CpG 1018 showed marginal adjuvant effects (**Fig. 4B**). The neutralizing activity of serum  
194 antibodies after the boost was measured in a pseudo-particle neutralization assay at Nexelis (part of CEPI's  
195 global network of laboratories to centralize assessment COVID-19 vaccine candidates) (15). Neutralization  
196 titers of hamster sera were substantially higher than those of human convalescent sera used as controls in  
197 the same assay (**Fig. 4C**). After challenge, we observed that animals which were immunized with all three  
198 vaccines without the adjuvant developed a similar trend of body weight change. Animals that were  
199 immunized with GPO and Butantan vaccines in the presence of the CpG 1018 showed improved protection  
200 manifested by less weight loss. The adjuvant did not seem to alleviate body weight loss of animals that  
201 received the IVAC vaccine (**Fig. 4D**). This observation is consistent with the post-boost antibody level  
202 (D33) (**Fig. 4B**). Nevertheless, all the animals that were vaccinated with NDV-HXP-S developed immunity  
203 to inhibit SARS-CoV-2 replication in the lungs showing no detectable infectious viral titers (**Fig. 4E**). In  
204 the nasal washes of vaccinated animals, virus shedding was significantly reduced in contrast to that in the

205 negative control animals (**Fig. 4F**). Virus was still able to replicate in the nasal turbinates of all infected  
206 animals, but all NDV-HXP-S vaccinated animals showed a reduced viral load (**Fig. 4G**). To evaluate  
207 SARS-CoV-2 induced lung disease, the left lung lobes were collected at day 5 post-challenge and processed  
208 for histopathology analysis. As expected, much less pathological change reflecting injury or inflammation  
209 was observed in the lungs of NDV-HXP-S vaccinated animals as compared to those in the lungs of  
210 negative control animals (**Fig. S2**). In conclusion, inactivated NDV-HXP-S vaccine prepared by three egg-  
211 based influenza virus vaccine manufacturers showed equally good efficacy at inducing binding/neutralizing  
212 antibodies, inhibiting virus replication and shedding as well as minimizing SARS-CoV-2 induced lung  
213 pathology in hamsters. An FDA approved adjuvant, CpG 1018 mildly increased protection from body  
214 weight loss of hamsters after challenge.

215

### 216 **Live NDV-HXP-S protects hamsters and mice from SARS-CoV-2 challenge**

217 While there is no attenuated SARS-CoV-2 available as a live vaccine, live viral vector COVID-19  
218 vaccines were rapidly developed in several platforms. In addition to adenovirus vectors, paramyxovirus  
219 vectors have been used such as measles virus (16) and Newcastle disease virus (2, 3, 17). Live vaccines  
220 typically would have an advantage over inactivated vaccine at inducing strong local innate immune  
221 responses, T-cell responses and sterilizing mucosal antibody responses – especially when administered  
222 mucosally. To reiterate that the design of the NDV-HXP-S renders versatility of the construct to be used as  
223 both inactivated and live vaccine, we evaluated NDV-HXP-S as a live vector vaccine in two preclinical  
224 animal models testing two different vaccination regimens. First, we examined two immunizations of live  
225 NDV-HXP-S via the intranasal route in the hamster model. NDV-HXP-S at a dose of  $10^6$  fifty percentage  
226 of egg embryo infectious dose (EID<sub>50</sub>) administered to hamsters intranasally twice at day 0 and day 22. A  
227 vector only control group was immunized with the same dose of WT NDV. A negative control group was  
228 mock-vaccinated with PBS. A healthy control group was kept unvaccinated (**Fig. 5A**). Serum IgG titer  
229 showed that one immunization was sufficient to induce potent binding antibody responses, while the booster  
230 vaccination did not further increase titers. We speculated that the booster vaccination might generate more  
231 mucosal immunity such as spike-specific IgA, which was not measured in this study (**Fig. 5B**). The  
232 neutralizing activity of post-boost sera was measured against the (WT) USA-WA1/2020, and the B.1.351  
233 and B.1.1.7 variants. A similar trend was observed as in previous studies, where immune sera neutralized  
234 the (WT) USA-WA1/2020 and the B.1.1.7 variant equally well and crossed-neutralized the B.1.351 variant  
235 with a reduced potency (**Fig. 5C**). Upon challenge with  $10^5$  PFU of the USA-WA1/2020 strain, we observed  
236 that the NDV-HXP-S vaccinated animals show no weight changes like the healthy control group, whereas  
237 the negative control group lost a substantial amount of weight by day 5. Animals vaccinated with the WT  
238 NDV exhibited weight loss that was less pronounced than that of the negative control group. This could

239 possibly be due to the innate antiviral response induced by the live WT NDV (**Fig. 5D**). At day 2 post  
240 infection, viruses were cleared in the lungs of animals that received the NDV-HXP-S, whereas both WT  
241 NDV and PBS groups showed similar high viral titers in the lung homogenates. In the nasal washes of WT  
242 NDV and PBS control animals, viral titers are comparably high, while only one animal out of three in the  
243 NDV-HXP-S group showed measurable viral titer (**Fig. 5E**). In summary, this study confirmed the  
244 effectiveness of the NDV-HXP-S as a live viral vector vaccine when administered intranasally. The vaccine  
245 not only prevented SARS-CoV-2 replication in the lungs but also significantly reduced virus shedding from  
246 the nasal cavity, which would greatly diminish the risk of virus transmission as well.

247 In addition to the hamster study testing only the intranasal route of the live vaccine, we performed  
248 a mouse study evaluating a different immunization regimen of the live NDV-HXP-S, combining the  
249 intranasal and intramuscular routes aiming to bring both mucosal and systemic immunity into action. Of  
250 note, the live nature of the NDV-HXP-S would have an adjuvant effect compared to an inactivated NDV-  
251 HXP-S. Here we examined this vaccination strategy with three different doses, in which the animals  
252 received the same titer of live NDV-HXP-S for the intranasal prime and the intramuscular boost. Three  
253 groups of animals were immunized with  $10^4$  EID<sub>50</sub>,  $10^5$  EID<sub>50</sub> and  $10^6$  EID<sub>50</sub> of NDV-HXP-S, respectively.  
254 A vector-only control group was immunized with  $10^6$  EID<sub>50</sub> of the WT NDV. The negative control group  
255 was mock-vaccinated with PBS. The two immunizations were 3 weeks apart. Mice were again sensitized  
256 with Ad5-hACE2 as described earlier and challenged with  $10^5$  PFU of the USA-WA1/2020 strain (**Fig. 6A**).  
257 By ELISA we observed a dose-dependent antibody titer, in which the high-dose group developed the  
258 strongest antibody responses after each immunization (**Fig. 6B**). IgG subclasses ELISAs showed a  
259 favorable induction of IgG2a over IgG1 in all NDV-HXP-S vaccine groups (**Fig. S1B**). As expected, mice  
260 vaccinated with the high-dose developed the highest level of neutralizing/cross-neutralizing antibodies to  
261 the WT and variant SARS-CoV-2 (**Fig. 6C**). In terms of protection, a reverse correlation of the vaccine  
262 dose and viral load in the lung homogenates was observed (**Fig. 6D**); the high-dose regimen conferred the  
263 best protection among the three groups. A duplicate experiment including the high dose-group ( $10^6$  EID<sub>50</sub>  
264 of NDV-HXP-S) and vector-only control group ( $10^6$  EID<sub>50</sub> of WT NDV) were set up to measure spike-  
265 specific IgA in the nasal washes, which were collected 21 days after intranasal prime. A spike-specific IgA  
266 ELISA showed that animals which received the NDV-HXP-S developed IgA on their respiratory mucosal  
267 surfaces (**Fig. S3**).

268

### 269 **NDV-HXP-S is effective against SARS-CoV-2 variants of concern in the mouse model**

270 With the emergence of variants of concern that are partially resistant to NAbs raised against the  
271 WT SARS-CoV-2 attributed to the amino acid substitutions or deletions in the N-terminal domain (NTD)  
272 and the receptor-binding domain (RBD), we performed vaccination in mice with inactivated NDV-HXP-S

273 and challenged them with USA-WA1/2020, hCoV-19/USA/MD-HP01542/2021 JHU (B.1.351) and hCoV-  
274 19/Japan/TY7-503/2021 (P.1) after Ad5-hACE2 treatment. This was to ensure efficient replication of all  
275 three viruses, although both B.1.351 and P.1 variants have been reported to extend their host tropism to  
276 murine ACE2 (18). The vaccination group received intramuscular injection of 1 µg of inactivated NDV-  
277 HXP-S, while the negative control group received 1 µg of the inactivated WT NDV. Two doses were  
278 administered, 3 weeks apart. One third of the mice from each group was challenged with USA-WA1/2020,  
279 hCoV-19/USA/MD-HP01542/2021 JHU (B.1.351) and hCoV-19/Japan/TY7-503/2021 (P.1), respectively.  
280 Lungs of animals from each group were harvested at day 2. Viral loads were measured as described earlier.  
281 The NDV-HXP-S reproducibly inhibited WT virus replication to a great magnitude, while it also reduced  
282 B.1.351 replication by a factor of ~1000 and P.1 replication by a factor of ~280 at day 2 post-challenge  
283 (Fig 7). This study demonstrated that with expected reduction to neutralize the variants of concern, NDV-  
284 HXP-S is still effective at robustly inhibiting virus replication *in vivo*, which would be essential to mitigate  
285 disease.

286  
287

## 288 Discussion

289 The COVID-19 pandemic has promoted the unprecedented development of various vaccine  
290 platforms from the conventional inactivated whole-virion vaccines, to novel mRNA vaccines, recombinant  
291 protein subunit vaccines and viral vector vaccines (19). The high efficacy of some novel vaccines is not  
292 necessarily followed by universal accessibility, due to logistical barriers (e.g. cost, manufacturing  
293 infrastructure, supply of raw materials, production capacity, transportation/storage and distribution).  
294 Newcastle disease virus was identified as an avian pathogen in the 1920's, and was later developed as  
295 oncolytic agent and veterinary vaccine using non-virulent strains (20-25). Similar to many other  
296 paramyxoviruses, NDV tolerates large insertions and has been evaluated as vaccine vector for a number of  
297 animal pathogens in preclinical studies (22, 25-33). To increase the surface expression of the inserted gene,  
298 the transmembrane domain and cytoplasmic tail of the target membrane protein can be replaced by that of  
299 HN or F protein of NDV (32). Using this strategy, we have previously constructed a viral vector (NDV  
300 expressing the S-F chimera) and shown that it can be used as an inactivated vaccine against SARS-CoV-2  
301 (2). This construct was later optimized to further stabilize the S-F by introducing HexaPro mutations  
302 identified via structural biology (34). This second generation NDV-HXP-S was quickly developed and is  
303 currently being evaluated in Phase I clinical trials in Mexico (NCT04871737, live vaccine), Vietnam  
304 (NCT04830800, inactivated vaccine) and Thailand (NCT04764422, inactivated vaccine).

305 While the clinical trials are ongoing, we demonstrate here the versatility of the NDV-HXP-S in  
306 preclinical studies using mice and hamsters stressing its effectiveness as a live vaccine or an inactivated

307 vaccine. The live nature of the vaccine allowed for mucosal administration as well as intramuscular  
308 administration. There is also an important manufacturing consideration differentiating the live NDV  
309 vaccine from the inactivated vaccine technology. Live vaccine for humans must be propagated in specific  
310 pathogen free (SPF) embryonated eggs, while inactivated vaccine for humans can be safely manufactured  
311 in non-SPF eggs, as the inactivating process eliminates the risk of avian adventitious agents arising from  
312 the use of widely available breeder chicken eggs that are one tenth the cost and not limited in supply. A  
313 dose-ranging study in mice indicated the inactivated NDV-HXP-S was highly immunogenic even at a dose  
314 as low as 0.01  $\mu\text{g}$  of the total protein (the amount of the spike protein would be much less). The adjuvant  
315 CpG 1018 leads to an antigen-sparing effect which is slightly better in mice than that in hamsters. It was  
316 postulated that the NDV could be self-adjuvanting due to viral components (RNA and proteins) being  
317 present, resulting in less beneficial effect of the adjuvant. However, we did observe that CpG 1018 drove a  
318 more prominent IgG2a production over IgG1 than the unadjuvanted vaccine in mice, suggesting it could  
319 promote a favorable  $T_{\text{H}1}$  response, which will be measured in the Phase I trials that include CpG 1018  
320 adjuvanted groups. The final verdict for the usefulness of CpG 1018 in combination with NDV-HXP-S will  
321 come from the human data. Moreover, it appeared that an oil-in-water nano-emulsion adjuvant (AddaVax)  
322 also enhanced antibody titers. It will be of great interest to evaluate other adjuvants in our future preclinical  
323 studies.

324 It was observed that mice and hamsters vaccinated with NDV-HXP-S developed strong antibody  
325 responses that not only neutralized the prototype SARS-CoV-2 but also cross-neutralized variants of  
326 interest/concern. The reduction of neutralizing activity against B.1.351 and B.1.1.7 is consistent with what  
327 was observed for other vaccines using the prototype spike as the immunogen (6-9). Interestingly, cross-  
328 neutralization was improved by using CpG 1018 as adjuvant. Challenge studies in Ad5-hACE2 sensitized  
329 mice using B.1.351 and P.1 variants demonstrated good protection by the prototype antigen expressed by  
330 the NDV. Last but not least, this NDV platform could be quickly adapted to express the spike protein of  
331 SARS-CoV-2 variants. So far, we have successfully generated NDV-HXP-S (B.1.351), NDV-HXP-S  
332 (B.1.1.7) and NDV-HXP-S (P.1) and are evaluating them in animal models. Heterologous vaccination  
333 regimens or multi-valent formulations might be beneficial to the induction of cross-protective antibodies.

334

335

## 336 **Materials and methods**

### 337 **Cells**

338 BSRT7 cells were a kind gift from Dr. Benhur Lee at Icahn School of Medicine at Mount Sinai  
339 (ISMMS) (35, 36) and Vero E6 cells were purchased from ATCC (CRL-1586). Chicken embryo fibroblasts  
340 (CEF) were isolated as described in a previous study (37). All cell lines were maintained in Dulbecco's

341 Modified Eagle's Medium (DMEM; Gibco) containing 10% (vol/vol) fetal bovine serum (FBS), 100  
342 unit/mL of penicillin, 100 µg/mL of streptomycin (P/S; Gibco) and 10 mM 4-(2-hydroxyethyl)-1-  
343 piperazineethanesulfonic acid (HEPES) at 37 °C with 5% CO<sub>2</sub>.

344

#### 345 **Plasmids**

346 HexaPro (HXP) mutations including F817P, A892P, A899P, A942P, K986P and V987P that have  
347 been identified to stabilize the prefusion conformation of spike (4) were introduced into the S-F chimera  
348 by PCR (HXP-S) (2). The sequence of the HXP-S was inserted into pNDV\_LS/L289A rescue plasmid  
349 (between P and M genes) by in-Fusion cloning (Clontech). The recombination product was transformed  
350 into MAX Efficiency™ Stbl2™ Competent Cells (Thermo Fisher Scientific) to generate the pNDV-HXP-  
351 S rescue plasmid. The plasmid was purified using PureLink™ HiPure Plasmid Maxiprep Kit (Thermo  
352 Fisher Scientific).

353

#### 354 **Rescue of the NDV-HXP-S**

355 As described in our previous studies (2), BSRT7 cells stably expressing the T7 polymerase were  
356 seeded onto 6-well plates at 3 x 10<sup>5</sup> cell per well in duplicate. The next day, cells were transfected with 2  
357 µg of pNDV-HXP-S, 1 µg of pTM1-NP, 0.5 µg of pTM1-P, 0.5 µg of pTM1-L and 1 µg of pCI-T7opt were  
358 re-suspended in 250 µL of Opti-MEM (Gibco). The plasmid cocktail was then gently mixed with 15 µL of  
359 TransIT LT1 transfection reagent (Mirus). The growth media were replaced with opti-MEM during  
360 transfection. To increase rescue efficiency, BSRT7-CEF co-culture was established the next day as  
361 described previously (38). Specifically, transfected BSRT7 cells and CEF wells were washed with warm  
362 PBS and trypsinized. Trypsinized cells were neutralized with excessive amount of growth media. Mix  
363 BSRT7 cells with CEF cells (~1: 2.5) in a 10-cm dish. The co-culture was incubated at 37°C overnight.  
364 The next day, the media were removed and cells were gently washed with warm PBS, opti-MEM  
365 supplemented with 1% P/S and 0.1 µg/mL of tosyl phenylalanyl chloromethyl ketone (TPCK)- treated  
366 trypsin was added. The co-cultures were incubated for 2 or 3 days before inoculation into 8 or 9 day-old  
367 embryonated chicken eggs. To inoculate eggs, cells and supernatants were harvested and homogenized by  
368 several syringe strokes. One or two hundred microliters of the mixture was injected into each egg. Eggs  
369 were incubated at 37 °C for 3 days and cooled at 4°C overnight. Allantoic fluid was harvested from cooled  
370 eggs and the rescue of the viruses was determined by hemagglutination (HA) assays.

371

372

#### 373 **Preparation of inactivated concentrated virus**

374 The viruses in the allantoic fluid were first inactivated using 0.05% beta-propiolactone (BPL) as  
375 described previously (2). To concentrate the viruses, allantoic fluids were clarified by centrifugation at  
376 4,000 rpm at 4°C for 30 min using a Sorvall Legend RT Plus Refrigerated Benchtop Centrifuge (Thermo  
377 Fisher Scientific). Clarified allantoic fluids were laid on top of a 20% sucrose cushion in NTE buffer (100  
378 mM NaCl, 10 mM Tris-HCl, 1 mM EDTA, pH 7.4). Ultracentrifugation in a Beckman L7-65 ultracentrifuge  
379 at 25,000 rpm for two hours at 4°C using a Beckman SW28 rotor (Beckman Coulter) was performed to  
380 pellet the viruses through the sucrose cushion while soluble egg proteins were removed. The virus pellets  
381 were re-suspended in PBS (pH 7.4). The total protein content was determined using the bicinchoninic acid  
382 (BCA) assay (Thermo Fisher Scientific).

383  
384

### 385 **SDS-PAGE**

386 The concentrated NDV-HXP-S or WT NDV was mixed with Novex™ Tris-Glycine SDS Sample  
387 Buffer (2X) (Thermo Fisher Scientific), NuPAGE™ Sample Reducing Agent (10 x) (Thermo Fisher  
388 Scientific) and PBS at appropriate amounts to reach a total protein content of 20 µg in 50 µl volume. The  
389 mixture was heated at 90 °C for 5 min. The samples were mixed by pipetting and loaded at 30 µg to a 4-  
390 20% 10-well Mini-PROTEAN TGX™ precast gel (Bio-Rad). Ten microliters of the Novex™ Sharp Pre-  
391 stained Protein standard (Thermo Fisher Scientific) was used as the ladder. The electrophoresis was run in  
392 Tris/Glycine SDS/Buffer (Bio-Rad). The gel was then washed with distilled water at room temperature  
393 several times until the dye front in the gel was no longer visible. The gel was stained with 20 mL of  
394 SimplyBlue™ SafeStain (Thermo Fisher Scientific) for a minimal of 1 hour to overnight. The  
395 SimplyBlue™ SafeStain was decanted and the gel was washed with distilled water several times until the  
396 background was clear. Gels were imaged using the Bio-Rad Universal Hood Ii Molecular imager (Bio-Rad)  
397 and processed by Image Lab Software (Bio-Rad).

398

### 399 **Virus titration by EID<sub>50</sub> assays**

400 Fifty percent of egg embryo infectious dose (EID<sub>50</sub>) assay was performed in 9 to 11-day old chicken  
401 embryonated eggs. Virus in allantoic fluid was 10-fold serially diluted in PBS, resulting in 10<sup>-5</sup> to 10<sup>-10</sup>  
402 dilutions of the virus. One hundred microliters of each dilution was injected into each egg for a total of 5-  
403 10 egg per dilution. The eggs were incubated at 37 °C for 3 days and then cooled at 4°C overnight. Allantoic  
404 fluids were collected and analyzed by HA assay. The EID<sub>50</sub> titer of the NDV, determined by the number of  
405 HA-positive and HA-negative eggs in each dilution was calculated using the Reed and Muench method.

406

### 407 **Animal experiments**

408 All the animal experiments were performed in accordance with protocols approved by the Icahn  
409 School of Medicine at Mount Sinai Institutional Animal Care and Use Committee (IACUC). All  
410 experiments with live SARS-CoV-2 were performed in the Centers for Disease Control and Prevention  
411 (CDC)/US Department of Agriculture (USDA)-approved biosafety level 3 (BSL-3) biocontainment facility  
412 of the Global Health and Emerging Pathogens Institute at the Icahn School of Medicine at Mount Sinai, in  
413 accordance with institutional biosafety requirements.

414

#### 415 **Mouse immunization and challenge studies**

416 Female BALB/c mice were used in all studies. For intramuscular vaccination using the inactivated  
417 NDV-HXP-S, vaccine or negative control WT NDV was prepared in 100  $\mu$ l total volume with or without  
418 CpG 1018 as the adjuvant. Two immunizations were performed for all the mice with a 21-day interval. To  
419 administer live NDV-HXP-S, mice were anesthetized with ketamine/xylazine cocktail and vaccinated with  
420 NDV-HXP-S, WT NDV or PBS in 30  $\mu$ l total volume via the intranasal route (IN) and boosted with the  
421 same preparation via the IM route with a 21-day interval. For SARS-CoV-2 infection, mice were  
422 intranasally infected with  $2.5 \times 10^8$  PFU of Ad5-hACE2 5 days prior to being challenged with  $10^5$  PFU of  
423 the USA-WA1/2020 strain,  $3.4 \times 10^4$  PFU of the hCoV-19/USA/MD-HP01542/2021 JHU strain (B.1.351,  
424 kindly provided by Dr. Andrew Pekosz from Johns Hopkins Bloomberg School of Public Health) or  $6.3 \times$   
425  $10^4$  PFU of the hCoV-19/Japan/TY7-503/2021 strain (P.1). Viral titers in the lung homogenates of mice 2  
426 days or 5 days post-infection were used as the readout for protection. Briefly, the lung lobes were harvested  
427 from a subset of animals per group and homogenized in 1 mL of sterile PBS. Viral titers in the lung  
428 homogenates were measured by plaque assay on Vero E6 cells. To collect nasal washes, mice were  
429 euthanized and nasal washes were collected in 1 mL PBS containing 0.1% BSA, 10 units/mL penicillin and  
430 10  $\mu$ g/mL streptomycin. The nasal washes were spun at 3,000 rpm for 20 min at 4°C and stored at -80°C.  
431 Blood was collected by submandibular vein bleeding. Sera were isolated by low-speed centrifugation and  
432 stored at -80°C until use.

433

#### 434 **Hamster immunization and challenge studies**

435 Female Golden Syrian hamsters were used in all the studies. For intramuscular vaccination study,  
436 NDV-HXP-S vaccine or negative control WT NDV/PBS was prepared in 100  $\mu$ L of total volume either  
437 without adjuvants, or with 100  $\mu$ g of CpG 1018 or 50  $\mu$ L of AddaVax as the adjuvant. For the intranasal  
438 vaccination study, hamsters were anesthetized with ketamine/xylazine cocktail before the intranasal  
439 administration of live NDV-HXP-S, WT NDV or PBS in a 50  $\mu$ L volume. An unvaccinated healthy control  
440 group was included in each study. The animals were vaccinated following a prime-boost regimen in a ~3-  
441 week interval. Two to three-weeks after the boost, animals were challenged with  $10^4$  or  $10^5$  PFU of the

442 USA-WA1/2020 strain, except that the healthy control group was mock-challenged with the same amount  
443 of PBS. Animals were bled via lateral saphenous vein and sera were isolated by low-speed centrifugation.  
444 Weight changes of the animals were monitored for 5 days. A subset of animals from each group was  
445 euthanized at day 2 and day 5 post-challenge to harvest lungs lobes (upper right lung lobe, lower right lung  
446 lobe), nasal turbinates or nasal washes. Each right lung lobe was homogenized in 1 mL of PBS. The nasal  
447 turbinates were homogenized in 0.5 mL of PBS. Nasal washes were collected in 0.4 mL PBS. Viral titers  
448 in the nasal washes, nasal turbinate and lung homogenates were measured by plaque assay on Vero E6 cells.  
449 The left lung lobes were collected at day 5 and fixed/perfused with neutral buffered formalin for  
450 histopathology. Of note, the challenge study using GMP vaccine from the three collaborating manufacturers  
451 was conducted using similar methods for assessments of outcomes, but with vaccine formulations from  
452 each manufacturer containing 1 µg of S protein per dose, with or without CpG 1018.

453

#### 454 **ELISAs**

455 ELISAs were performed as described previously (2, 3) to measure spike-specific IgG in the serum  
456 of mice and hamsters vaccinated with NDV-HXP-S. To measure spike-specific IgG1 or IgG2a subclass in  
457 the mouse sera, an HRP-conjugated goat anti-mouse IgG1 (ab97240, Abcam) or an HRP-conjugated goat  
458 anti-mouse IgG2a (ab97245, Abcam) were used at 1:3000 dilution. A starting dilution of 1: 30 was used  
459 for serum samples. To measure spike-specific IgA in the nasal wash, the clarified undiluted nasal washes  
460 were used and serially diluted by 2-fold. An HRP-conjugated goat anti-mouse IgA secondary antibody  
461 (PA1-74397 Invitrogen) was used at 1: 2000 dilution.

462

#### 463 **Microneutralization assays using the authentic SARS-CoV-2 viruses**

464 The microneutralization assays using the authentic SARS-CoV-2 viruses were described  
465 previously (39). To compare the neutralization titers of immune sera from animals vaccinated with NDV-  
466 HXP-S, the neutralization assays against the wild type SARS-CoV-2 (isolate USA-WA1/2020), hCoV-  
467 19/South Africa/KRISP-K005325/2020 (B.1.351, BEI Resources NR-54009) and hCoV-  
468 19/England/204820464/2020 (B.1.1.7, BEI Resources NR-54000) were performed at the same time to  
469 avoid assay-to-assay variations.

470

#### 471 **Pseudo-particle neutralization assays**

472 The pseudo-particle neutralization assay (PNA) was performed by Nexelis using a replication  
473 incompetent vesicular stomatitis virus (VSV) displaying the spike protein of Wuhan-Hu-1 strain (15).

474

#### 475 **SARS-CoV-2 plaque assay**

476 The plaque assay was performed in BSL3 facility. Vero E6 cells were seeded onto 12-well plates  
 477 in growth media at 1:5 and were cultured for two days. Tissue homogenates or nasal washes were 10-fold  
 478 serially diluted in infection medium (DMEM containing 2% FBS, P/S and 10 mM HEPES). Two hundred  
 479 microliters of each dilution were inoculated onto each well starting with 1:10 dilution of the sample. The  
 480 plates were incubated at 37 °C for 1 hour with occasional rocking every 10 minutes. The inoculum in each  
 481 well was then removed and 1 mL of agar overlay containing 0.7% of agar in 2 x MEM was placed onto  
 482 each well. Once the agar was solidified, the plates were incubated at 37 °C with 5% CO<sub>2</sub>. Two days later,  
 483 the plates were fixed with 5% formaldehyde in PBS overnight before being taken out of BSL3 for  
 484 subsequent staining in BSL2 cabinet. The plaques were immuno-stained with an anti-SARS-CoV-2 NP  
 485 primary mouse monoclonal antibody 1C7C7 kindly provided by Dr. Thomas Moran at ISMMS. An HRP-  
 486 conjugated goat anti-mouse secondary antibody was used at 1:2000 and the plaques were visualized using  
 487 TrueBlue™ Peroxidase Substrate (SeraCare Life Sciences Inc.).

488  
 489

490 **Histopathology**

491 Formalin-fixed, paraffin-embedded (FFPE) left lung tissues obtained from hamsters were cut into  
 492 5 µm sections and stained with hematoxylin and eosin (H&E) by the Biorepository and Pathology Core.  
 493 All sections were evaluated by a veterinary pathologist who was blinded to the vaccination groups in the  
 494 Comparative Pathology Laboratory (CPL) at ISMMS. The scoring system used was described in the table  
 495 below.

| Score | Area affected | Epithelial degeneration/necrosis  | Inflammation  |
|-------|---------------|---|---|
| 0     | none          | none  | None  |
| 1     | 5-10%         | Minimal; scattered cell necrosis/vacuolation affecting 5 to 10% of tissue section | Minimal; scattered inflammatory cells affecting 5-10% of tissue section |
| 2     | 10-25%        | Mild; scattered cell necrosis/vacuolation   | multifocal, few inflammatory cells                                      |
| 3     | 25-50%        | Moderate; multifocal vacuolation or sloughed/necrotic cells                       | Thin layer of cells (<5 cell layer thick)                               |

|     |   |        |   |   |
|-----|---|--------|---|---|
| 496 | 4 | 50-75% | Marked; multifocal/segmental<br>necrosis, epithelial<br>loss/effacement | Thick layer of cells (>5<br>cell layer thick) |
| 497 |   |        |   |   |
| 498 |   |        |   |   |
| 499 | 5 | >75%   | Severe; coalescing areas of<br>necrosis, parenchymal<br>effacement      | Confluent areas of<br>inflammation            |
| 500 |   |        |   |   |
| 501 |   |        |   |   |
| 502 |   |        |   |   |

503

504 **Statistical analysis**

505 The statistical analysis was performed using GraphPad Prism 7.0. For multiple comparison, the  
506 statistical difference was determined using ordinary one-way ANOVA or two-way ANOVA with Dunnett's  
507 correction. To compare two groups, a one-tailed t test was used.

508

509 **Data availability**

510 The data that support the findings of this study are available from the corresponding author upon  
511 reasonable request

512

513 **References**

514 1. Anonymous. 2021. Tracking Coronavirus Vaccination Around the World. The New York Times.

515 2. Sun W, McCroskery S, Liu WC, Leist SR, Liu Y, Albrecht RA, Slamanig S, Oliva J, Amanat F,  
516 Schafer A, Dinnon KH, 3rd, Innis BL, Garcia-Sastre A, Krammer F, Baric RS, Palese P. 2020. A  
517 Newcastle Disease Virus (NDV) Expressing a Membrane-Anchored Spike as a Cost-Effective  
518 Inactivated SARS-CoV-2 Vaccine. *Vaccines (Basel)* 8.

519 3. Sun W, Leist SR, McCroskery S, Liu Y, Slamanig S, Oliva J, Amanat F, Schafer A, Dinnon KH,  
520 3rd, Garcia-Sastre A, Krammer F, Baric RS, Palese P. 2020. Newcastle disease virus (NDV)  
521 expressing the spike protein of SARS-CoV-2 as a live virus vaccine candidate. *EBioMedicine*  
522 62:103132.

523 4. Hsieh CL, Goldsmith JA, Schaub JM, DiVenere AM, Kuo HC, Javanmardi K, Le KC, Wrapp D,  
524 Lee AG, Liu Y, Chou CW, Byrne PO, Hjorth CK, Johnson NV, Ludes-Meyers J, Nguyen AW,  
525 Park J, Wang N, Amengor D, Lavinder JJ, Ippolito GC, Maynard JA, Finkelstein IJ, McLellan JS.  
526 2020. Structure-based design of prefusion-stabilized SARS-CoV-2 spikes. *Science* 369:1501-  
527 1505.

528 5. Sparrow E, Wood JG, Chadwick C, Newall AT, Torvaldsen S, Moen A, Torelli G. 2021. Global  
529 production capacity of seasonal and pandemic influenza vaccines in 2019. *Vaccine* 39:512-520.

- 530 6. Shen X, Tang H, Pajon R, Smith G, Glenn GM, Shi W, Korber B, Montefiori DC. 2021.  
531 Neutralization of SARS-CoV-2 Variants B.1.429 and B.1.351. *N Engl J Med*  
532 doi:10.1056/NEJMc2103740.
- 533 7. Liu Y, Liu J, Xia H, Zhang X, Fontes-Garfias CR, Swanson KA, Cai H, Sarkar R, Chen W,  
534 Cutler M, Cooper D, Weaver SC, Muik A, Sahin U, Jansen KU, Xie X, Dormitzer PR, Shi PY.  
535 2021. Neutralizing Activity of BNT162b2-Elicited Serum. *N Engl J Med* 384:1466-1468.
- 536 8. Zhou D, Dejnirattisai W, Supasa P, Liu C, Mentzer AJ, Ginn HM, Zhao Y, Duyvesteyn HME,  
537 Tuekprakhon A, Nutalai R, Wang B, Paesen GC, Lopez-Camacho C, Slon-Campos J, Hallis B,  
538 Coombes N, Bewley K, Charlton S, Walter TS, Skelly D, Lumley SF, Dold C, Levin R, Dong T,  
539 Pollard AJ, Knight JC, Crook D, Lambe T, Clutterbuck E, Bibi S, Flaxman A, Bittaye M, Belij-  
540 Rammerstorfer S, Gilbert S, James W, Carroll MW, Klenerman P, Barnes E, Dunachie SJ, Fry  
541 EE, Mongkolsapaya J, Ren J, Stuart DI, Sreaton GR. 2021. Evidence of escape of SARS-CoV-2  
542 variant B.1.351 from natural and vaccine-induced sera. *Cell* 184:2348-2361 e6.
- 543 9. Hoffmann M, Arora P, Gross R, Seidel A, Hornich BF, Hahn AS, Kruger N, Graichen L,  
544 Hofmann-Winkler H, Kempf A, Winkler MS, Schulz S, Jack HM, Jahrsdorfer B, Schrezenmeier  
545 H, Muller M, Kleger A, Munch J, Pohlmann S. 2021. SARS-CoV-2 variants B.1.351 and P.1  
546 escape from neutralizing antibodies. *Cell* 184:2384-2393 e12.
- 547 10. Rathnasinghe R, Strohmeier S, Amanat F, Gillespie VL, Krammer F, Garcia-Sastre A, Coughlan  
548 L, Schotsaert M, Uccellini MB. 2020. Comparison of transgenic and adenovirus hACE2 mouse  
549 models for SARS-CoV-2 infection. *Emerg Microbes Infect* 9:2433-2445.
- 550 11. Campbell JD. 2017. Development of the CpG Adjuvant 1018: A Case Study. *Methods Mol Biol*  
551 1494:15-27.
- 552 12. Stevens TL, Bossie A, Sanders VM, Fernandez-Botran R, Coffman RL, Mosmann TR, Vitetta  
553 ES. 1988. Regulation of antibody isotype secretion by subsets of antigen-specific helper T cells.  
554 *Nature* 334:255-8.
- 555 13. Jangra S, Ye C, Rathnasinghe R, Stadlbauer D, Personalized Virology Initiative study g,  
556 Krammer F, Simon V, Martinez-Sobrido L, Garcia-Sastre A, Schotsaert M. 2021. SARS-CoV-2  
557 spike E484K mutation reduces antibody neutralisation. *Lancet Microbe* doi:10.1016/S2666-  
558 5247(21)00068-9.
- 559 14. Xie X, Liu Y, Liu J, Zhang X, Zou J, Fontes-Garfias CR, Xia H, Swanson KA, Cutler M, Cooper  
560 D, Menachery VD, Weaver SC, Dormitzer PR, Shi PY. 2021. Neutralization of SARS-CoV-2  
561 spike 69/70 deletion, E484K and N501Y variants by BNT162b2 vaccine-elicited sera. *Nat Med*  
562 27:620-621.

- 563 15. Kumar A, Bernasconi V, Manak M, de Almeida Aranha AP, Kristiansen PA. 2021. The CEPI  
564 centralised laboratory network: supporting COVID-19 vaccine development. *Lancet* 397:2148-  
565 2149.
- 566 16. Lu M, Dravid P, Zhang Y, Trivedi S, Li A, Harder O, Kc M, Chaiwatpongsakorn S, Zani A,  
567 Kenney A, Zeng C, Cai C, Ye C, Liang X, Shimamura M, Liu SL, Mejias A, Ramilo O, Boyaka  
568 PN, Qiu J, Martinez-Sobrido L, Yount JS, Peeples ME, Kapoor A, Niewiesk S, Li J. 2021. A safe  
569 and highly efficacious measles virus-based vaccine expressing SARS-CoV-2 stabilized prefusion  
570 spike. *Proc Natl Acad Sci U S A* 118.
- 571 17. Rohaim MA, Munir M. 2020. A Scalable Topical Vectored Vaccine Candidate against SARS-  
572 CoV-2. *Vaccines (Basel)* 8.
- 573 18. Xavier Montagnetelli MP, Laurine Levillayer, Eduard Baquero Salazar, Grégory Jouvion, Laurine  
574 Conquet, Flora Donati, Mélanie Albert, Fabiana Gambaro, Sylvie Behillil, Vincent Enouf,  
575 Dominique Rousset, Jean Jaubert, Felix Rey, Sylvie van der Werf, View ORCID ProfileEtienne  
576 Simon-Loriere. 2021. The B.1.351 and P.1 variants extend SARS-CoV-2 host range to mice.  
577 *bioRxiv* doi:<https://doi.org/10.1101/2021.03.18.436013>.
- 578 19. Krammer F. 2020. SARS-CoV-2 vaccines in development. *Nature* doi:10.1038/s41586-020-2798-  
579 3.
- 580 20. Vijayakumar G, Zamarin D. 2020. Design and Production of Newcastle Disease Virus for  
581 Intratumoral Immunomodulation. *Methods Mol Biol* 2058:133-154.
- 582 21. Vijayakumar G, Palese P, Goff PH. 2019. Oncolytic Newcastle disease virus expressing a  
583 checkpoint inhibitor as a radioenhancing agent for murine melanoma. *EBioMedicine* 49:96-105.
- 584 22. Schirmacher V. 2016. Fifty Years of Clinical Application of Newcastle Disease Virus: Time to  
585 Celebrate! *Biomedicines* 4.
- 586 23. Zamarin D, Palese P. 2012. Oncolytic Newcastle disease virus for cancer therapy: old challenges  
587 and new directions. *Future Microbiol* 7:347-67.
- 588 24. Steel J, Burmakina SV, Thomas C, Spackman E, Garcia-Sastre A, Swayne DE, Palese P. 2008. A  
589 combination in-ovo vaccine for avian influenza virus and Newcastle disease virus. *Vaccine*  
590 26:522-31.
- 591 25. Ma J, Lee J, Liu H, Mena I, Davis AS, Sunwoo SY, Lang Y, Duff M, Morozov I, Li Y, Yang J,  
592 Garcia-Sastre A, Richt JA, Ma W. 2017. Newcastle disease virus-based H5 influenza vaccine  
593 protects chickens from lethal challenge with a highly pathogenic H5N2 avian influenza virus.  
594 *NPJ Vaccines* 2:33.

- 595 26. Grieves JL, Yin Z, Garcia-Sastre A, Mena I, Peeples ME, Risman HP, Federman H, Sandoval  
596 MJ, Durbin RK, Durbin JE. 2018. A viral-vectored RSV vaccine induces long-lived humoral  
597 immunity in cotton rats. *Vaccine* 36:3842-3852.
- 598 27. Liu RQ, Ge JY, Wang JL, Shao Y, Zhang HL, Wang JL, Wen ZY, Bu ZG. 2017. Newcastle  
599 disease virus-based MERS-CoV candidate vaccine elicits high-level and lasting neutralizing  
600 antibodies in Bactrian camels. *J Integr Agric* 16:2264-2273.
- 601 28. Maamary J, Array F, Gao Q, Garcia-Sastre A, Steinman RM, Palese P, Nchinda G. 2011.  
602 Newcastle disease virus expressing a dendritic cell-targeted HIV gag protein induces a potent  
603 gag-specific immune response in mice. *J Virol* 85:2235-46.
- 604 29. Carnero E, Li W, Borderia AV, Moltedo B, Moran T, Garcia-Sastre A. 2009. Optimization of  
605 human immunodeficiency virus gag expression by newcastle disease virus vectors for the  
606 induction of potent immune responses. *J Virol* 83:584-97.
- 607 30. Gao Q, Park MS, Palese P. 2008. Expression of transgenes from newcastle disease virus with a  
608 segmented genome. *J Virol* 82:2692-8.
- 609 31. DiNapoli JM, Kotelkin A, Yang L, Elankumaran S, Murphy BR, Samal SK, Collins PL,  
610 Bukreyev A. 2007. Newcastle disease virus, a host range-restricted virus, as a vaccine vector for  
611 intranasal immunization against emerging pathogens. *Proc Natl Acad Sci U S A* 104:9788-93.
- 612 32. Park MS, Steel J, Garcia-Sastre A, Swayne D, Palese P. 2006. Engineered viral vaccine  
613 constructs with dual specificity: avian influenza and Newcastle disease. *Proc Natl Acad Sci U S*  
614 *A* 103:8203-8.
- 615 33. Nakaya T, Cros J, Park MS, Nakaya Y, Zheng H, Sagrera A, Villar E, Garcia-Sastre A, Palese P.  
616 2001. Recombinant Newcastle disease virus as a vaccine vector. *J Virol* 75:11868-73.
- 617 34. Hsieh CL, Goldsmith JA, Schaub JM, DiVenere AM, Kuo HC, Javanmardi K, Le KC, Wrapp D,  
618 Lee AG, Liu Y, Chou CW, Byrne PO, Hjorth CK, Johnson NV, Ludes-Meyers J, Nguyen AW,  
619 Park J, Wang N, Amengor D, Maynard JA, Finkelstein IJ, McLellan JS. 2020. Structure-based  
620 Design of Prefusion-stabilized SARS-CoV-2 Spikes. *bioRxiv* doi:10.1101/2020.05.30.125484.
- 621 35. Buchholz UJ, Finke S, Conzelmann KK. 1999. Generation of bovine respiratory syncytial virus  
622 (BRSV) from cDNA: BRSV NS2 is not essential for virus replication in tissue culture, and the  
623 human RSV leader region acts as a functional BRSV genome promoter. *J Virol* 73:251-9.
- 624 36. Beaty SM, Park A, Won ST, Hong P, Lyons M, Vigant F, Freiberg AN, tenOever BR, Duprex  
625 WP, Lee B. 2017. Efficient and Robust Paramyxoviridae Reverse Genetics Systems. *mSphere* 2.
- 626 37. Hernandez R, Brown DT. 2010. Growth and maintenance of chick embryo fibroblasts (CEF).  
627 *Curr Protoc Microbiol* Appendix 4:4I.

- 628 38. Ayllon J, Garcia-Sastre A, Martinez-Sobrido L. 2013. Rescue of recombinant Newcastle disease  
629 virus from cDNA. *J Vis Exp* doi:10.3791/50830.
- 630 39. Amanat F, White KM, Miorin L, Strohmeier S, McMahon M, Meade P, Liu WC, Albrecht RA,  
631 Simon V, Martinez-Sobrido L, Moran T, Garcia-Sastre A, Krammer F. 2020. An In Vitro  
632 Microneutralization Assay for SARS-CoV-2 Serology and Drug Screening. *Curr Protoc*  
633 *Microbiol* 58:e108.

634

### 635 **Acknowledgements**

636 We thank Dr. Benhur Lee to kindly share the BSRT7 cells. We thank Dr. Thomas Moran for the 1C7C7  
637 antibody. We thank Dr. Robert Coffman and Dynavax for providing the CpG 1018. We thank Dr. Andrew  
638 Pekosz from Johns Hopkins Bloomberg School of Public Health for providing the B.1.351 challenge  
639 virus. We thank Dr. Randy Albrecht for support with the BSL3 facility and procedures at the Icahn  
640 School of Medicine at Mount Sinai, New York. We also thank Nexelis for performing the pseudo-particle  
641 neutralization assay. This work was partially supported by an NIAID funded Center of Excellence for  
642 Influenza Research and Surveillance (CEIRS, HHSN272201400008C, P.P.) and a grant from an  
643 anonymous philanthropist to Mount Sinai (PP, FK, AG-S). This work was also supported, in part, by the  
644 Bill & Melinda gates Foundation [INV-021239]. Under the grant conditions of the foundation, a Creative  
645 Commons Attribution 4.0 generic License has already been assigned to the Author Accepted Manuscript  
646 version that might arise from this submission. KS is supported by the Japanese Society for the Promotion  
647 of Science (JSPS) Overseas Research Fellowship.

648

649

### 650 **Author contributions**

651 Conceptualization and design: PP, FK, AG-S. and WS; construction and preparation of the vaccines: WS,  
652 SM, YL, SS, IGD; GMP lots vaccine preparation: IVAC, GPO, Instituto Butantan, PATH; mouse  
653 immunization and in vitro serological assays: WS, YL, IGD, KS ; mouse and hamster challenge and plaque  
654 assays: WS, YL, IGD; micro-neutralization assay: FA; data analysis: PP, WS, YL, IDG, FA, AG-S, FK;  
655 virus reagents: FA, LC, MS, IM, RR, SJ; first draft of the manuscript: PP and WS; manuscript review and  
656 editing, all authors.

657

### 658 **Competing interests**

659 The Icahn School of Medicine at Mount Sinai has filed patent applications entitled “RECOMBINANT  
660 NEWCASTLE DISEASE VIRUS EXPRESSING SARS-COV-2 SPIKE PROTEIN AND USES  
661 THEREOF” which names PP, FK, WS and AG-S. as inventors. The AG-S laboratory has received research

662 support from Pfizer, Senhwa Biosciences, Kenall Manufacturing, Avimex, Johnson & Johnson, Dynavax,  
663 7Hills Pharma, Pharmamar, ImmunityBio, Accurius, Merck and Nanocomposix, and AG-S has consulting  
664 agreements for the following companies involving cash and/or stock: Vivaldi Biosciences, Contrafect,  
665 7Hills Pharma, Avimex, Vaxalto, Pagoda, Accurius, Esperovax, Farmak, Applied Biological Laboratories  
666 and Pfizer.

667

668

## 669 **Figure legends**

670 **Figure .1 Design of the NDV-HXP-S construct. (A)** Structure and design of the NDV-HXP-S genome.

671 The ectodomain of the spike was connected to the transmembrane domain and cytoplasmic tail (TM/CT)  
672 of the F protein. The original polybasic cleavage site was removed by mutating RRAR to A. The HexaPro  
673 (F817P, A892P, A899P, A942P, K986P and V987P) stabilizing mutations were introduced. The sequence  
674 was codon-optimized for mammalian host expression **(B)** Protein staining of NDV-HXP-S. WT NDV as  
675 well as NDV-HXP-S were partially-purified from allantoic fluid through a sucrose cushion and  
676 resuspended in PBS. Five  $\mu\text{g}$  (1) and ten  $\mu\text{g}$  (2) of the WT NDV, as well as ten  $\mu\text{g}$  of NDV-HXP-S were  
677 resolved on 4-20% SDS-PAGE. The viral proteins were visualized by Coomassie Blue staining (L, S,  
678 HN, N, P and M).

679

680 **Figure 2. Low doses of inactivated NDV-HXP-S induce protective antibody response in mice. (A)**

681 Design of the study. Nine to ten-week old female BALB/c mice were used. Group 1 to 5 were vaccinated  
682 with unadjuvanted NDV-HXP-S at 1  $\mu\text{g}$ , 0.3  $\mu\text{g}$ , 0.1  $\mu\text{g}$ , 0.03  $\mu\text{g}$  and 0.01  $\mu\text{g}$  per mouse, respectively.  
683 Group 6 and 7 were vaccinated with 0.1  $\mu\text{g}$  of NDV-HXP-S with 10 or 30  $\mu\text{g}$  of CpG 1018 per mouse,  
684 respectively. Group 8 and 9 were vaccinated with 0.03  $\mu\text{g}$  of NDV-HXP-S with 10 or 30  $\mu\text{g}$  of CpG 1018  
685 per mouse, respectively. Group 10 was vaccinated with 1  $\mu\text{g}$  of WT NDV as the negative control. The  
686 vaccine was administered via the intramuscular (I.M.) route at D0 and D21. Blood was collected at D21  
687 and D43. Mice were sensitized with Ad5-hACE2 at D45 and challenged with  $10^5$  PFU of the USA-  
688 WA1/2020 strain. **(B)** Spike-specific serum IgG. Antibodies in post-prime (D21) and post-boost (D43)  
689 sera were measured by ELISAs. Geometric mean titer (GMT) represented by area under the curve (AUC)  
690 was graphed. **(C)** Neutralizing activity of serum antibodies. Post-boost sera from group 1, group 7 and  
691 group 10 were pooled within each group and tested in neutralization assays against the USA-WA1/2020  
692 strain (WT), the B.1.351 variant and B 1.1.7 variant in technical duplicate. Serum dilutions inhibiting  
693 50% of the infection ( $\text{ID}_{50}$ ) were plotted. (LoD: limit of detection; LoD=1:20; An  $\text{ID}_{50}$ =1:10 was assigned  
694 to negative samples) **(D)** Viral load in the lungs. Lungs of a subset of animals (n=4) from each group  
695 were collected at day 2 and day 5 post-challenge. The whole lungs were homogenized in 1 mL of PBS.

696 Viral titers were measured by plaque assay on Vero E6 cells and plotted as GMT of PFU/mL. (LoD=50  
697 PFU/mL; A titer of 25 PFU/mL was assigned to negative samples). Statistical difference was analyzed by  
698 ordinary one-way ANOVA corrected for Dunnett's multiple comparisons test (\*\*\*\*, <0.0001)

699

700 **Figure 3. Inactivated NDV-HXP-S induces protective antibody response in hamsters.** (A) Design of  
701 the study. Eighteen to twenty- week old female Golden Syrian hamsters were used. Group 1 to 3 were  
702 vaccinated with 5 µg of NDV-HXP-S without adjuvants, with CpG 1018 and AddaVax, respectively.  
703 Group 4 was vaccinated with 5 µg of WT NDV as the negative control. Group 5 was not vaccinated. The  
704 vaccine was administered via the intramuscular (I.M.) route at D0 and D21. Blood was collected at D21  
705 and D39. Group 1-4 were challenged with 10<sup>4</sup> PFU of USA-WA1/2020 strain at D42. Group 5 was mock-  
706 challenged with PBS. (B) Spike-specific serum IgG. Antibodies in post-prime (D21) and post-boost  
707 (D39) sera were measured by ELISAs. GMT endpoint titer was graphed. (C) Neutralizing activity of  
708 serum antibodies. Post-boost sera from group 1-4 were pooled within each group and tested in  
709 neutralization assays against USA-WA/2020 strain (WT), B.1.351 variant and B 1.1.7 variant in technical  
710 duplicate. Serum dilutions inhibiting 50% of the infection (ID<sub>50</sub>) were plotted. (LoD=1:50; An ID<sub>50</sub>=1:25  
711 was assigned to negative samples) (D) Body weight change of hamsters. Body weights were recorded for  
712 5 days after challenge. (E) Viral load in the lungs and nasal washes. Lower right and upper right lung  
713 lobes of a subset of animals (n=4 for group 1-4; n=3 for group 5) from each group were collected at day 2  
714 and day 5 post-challenge. Each lung lobe was homogenized in 1 mL PBS. Nasal washes were collected in  
715 0.4 mL of PBS. Viral titers were measured by plaque assay on Vero E6 cells and plotted as GMT of  
716 PFU/mL (LoD=50 PFU/mL; A titer of 25 PFU/mL was assigned to negative samples). Statistical  
717 difference was analyzed by two-way ANOVA corrected for Dunnett's multiple comparisons test (\*\*,  
718 p<0.005;\*\*\*, p<0.0005; \*\*\*\*, <0.0001)

719

720

721 **Figure 4. GMP lots of inactivated NDV-HXP-S produced by influenza virus vaccine manufacturers**  
722 **induce protective antibody response in hamsters.** (A) Design of the study. Nine to eleven-week old  
723 female Golden Syrian hamsters were used. Group 1 to 6 were vaccinated with 1 µg of spike antigen of  
724 inactivated NDV-HXP-S from GPO, IVAC and Butantan in the absence or presence of CpG 1018. Group  
725 7 was vaccinated with PBS as the negative control. Group 8 was not vaccinated (HC, healthy controls).  
726 The vaccine was administered via the intramuscular (I.M.) route at D0 and D21. Blood was collected at  
727 D0, D21 and D33. Group 1-7 were challenged with 10<sup>4</sup> PFU of the USA-WA1/2020 strain at D35. Group  
728 8 was mock-challenged with PBS. (B) Spike-specific serum IgG. Antibodies in pre-vaccination (D0),  
729 post-prime (D21) and post-boost (D33) sera were measured by ELISAs. GMT endpoint titers were

730 graphed. (C) Neutralizing activity of serum antibodies. Pseudo-particle neutralization assay was  
731 performed by Nexelis to measure neutralization titers of post-boost sera (D33). Human convalescent sera  
732 were included in the same assay as the controls (LoD=1:25; An ID<sub>50</sub>=1:12.5 was assigned to negative  
733 samples). (D) Body weight changes of hamsters. Body weights were monitored for 5 days after challenge.  
734 (E) Viral load in the lungs. Lower right and upper right Lung lobes of a subset of animals (n=4) from  
735 each group were collected at day 2 and day 5 post-challenge. Each lung lobe was homogenized in 1 mL  
736 PBS. (F) Viral load in nasal washes and nasal turbinates. At day 2 and day 5 post-challenge, nasal washes  
737 were collected in 0.4 mL of PBS. Nasal turbinates were homogenized in 0.5 mL PBS. Viral titers were  
738 measured by plaque assay on Vero E6 cells and plotted as GMT of PFU/mL (LoD=50 PFU/mL; A titer of  
739 25 PFU/mL was assigned to negative samples). Statistical difference was analyzed by ordinary one-way  
740 ANOVA corrected for Dunnett's multiple comparisons test (\*\*\*\*, p<0.0001)

741  
742

743 **Figure 5. Live NDV-HXP-S via the intranasal route induces protective antibody responses in**  
744 **hamsters.** (A) Design of the study. Eighteen to twenty- week old female Golden Syrian hamsters were  
745 used. Group 1 was vaccinated with 10<sup>6</sup> EID<sub>50</sub> of live NDV-HXP-S. Group 2 was vaccinated with 10<sup>6</sup>  
746 EID<sub>50</sub> of live WT NDV as the vector-only control. Group 3 was vaccinated with PBS as the negative  
747 control. Group 4 were the healthy controls. The vaccine was administered via the intranasal (I.N.) route at  
748 D0 and D22. Blood was collected at D22 and D41. Group 1-3 were challenged with 10<sup>5</sup> PFU of the USA-  
749 WA1/2020 strain at D44. Group 4 was mock-challenged with PBS. (B) Spike-specific serum IgG.  
750 Antibodies in post-prime (D22) and post-boost (D41) sera were measured by ELISAs. GMT endpoint  
751 titers were graphed. (C) Neutralizing activity of serum antibodies. Post-boost sera from group 1-3 were  
752 pooled within each group and tested in neutralization assay against USA-WA/2020 strain (WT), B.1.351  
753 variant and B 1.1.7 variant in technical duplicate. Serum dilutions inhibiting 50% of the infection (ID<sub>50</sub>)  
754 were plotted (LoD=1:50; An ID<sub>50</sub>=1:25 was assigned to negative samples). (D) Body weight change of  
755 hamsters. Body weight was recorded for 5 days after challenge. (E) Viral load in the lungs and nasal  
756 washes. Lower right and upper right lung lobes of a subset of animals (n=3) from each group were  
757 collected at day 2 and day 5 post-challenge. Each lung lobe was homogenized in 1 mL PBS. Nasal washes  
758 were collected in 0.4 mL of PBS. Viral titers were measured by plaque assay on Vero E6 cells and plotted  
759 as GMT of PFU/mL (LoD=50 PFU/mL; A titer of 25 PFU/mL was assigned to negative samples).  
760 Statistical difference was analyzed by two-way ANOVA corrected for Dunnett's multiple comparisons  
761 test (\*\*, p<0.005;\*\*\*, p<0.0005)

762  
763

764 **Figure 6. Intranasal prime followed by intramuscular boost of live NDV-HXP-S induces protective**  
765 **antibody responses in mice.** (A) Design of the study. Seven to nine- week-old female BALB/c mice  
766 were used. Group 1-3 were vaccinated with  $10^4$ ,  $10^5$  and  $10^6$  EID<sub>50</sub> of live NDV-HXP-S, respectively.  
767 Group 4 was vaccinated with  $10^6$  EID<sub>50</sub> of WT NDV. Group 5 was mock-vaccinated with PBS. The  
768 vaccine was administered via the intranasal (I.N.) route at D0 and intramuscular (I.M.) route at D21.  
769 Blood was collected at D21 and D43. Mice were sensitized with Ad5-hACE2 at D40 and challenged with  
770  $10^5$  PFU of the USA-WA1/2020 strain at D45. (B) Spike-specific serum IgG. Antibodies in post-prime  
771 (D21) and post-boost (D43) sera were measured by ELISAs. GMT AUC was graphed. (C) Neutralizing  
772 activity of serum antibodies. Post-boost sera from group 1-4 were pooled within each group and tested in  
773 neutralization assay against USA-WA/2020 strain (WT), B.1.351 variant and B.1.1.7 variant in technical  
774 duplicate. Serum dilutions inhibiting 50% of the infection (ID<sub>50</sub>) were plotted (LoD=1:50; An ID<sub>50</sub>=1:25  
775 was assigned to negative samples). (D) Viral load in the lungs. Lungs of a subset of animals (n=5) from  
776 each group were collected at day 2 and day 5 post-challenge. The whole lungs were homogenized in 1 mL  
777 PBS. Viral titers were measured by plaque assay on Vero E6 cells and plotted as GMT of PFU/mL  
778 (LoD=50 PFU/mL; A titer of 25 PFU/mL was assigned to negative samples). Statistical difference was  
779 analyzed by ordinary one-way ANOVA corrected for Dunnett's multiple comparisons test (\*\*\*\*,  
780 <0.0001)

781  
782 **Figure 7. Inactivated NDV-HXP-S induces protective antibody response against challenge of SARS-**  
783 **CoV-2 variants of concern.** Eight to ten- week-old female BALB/c mice were either vaccinated with 1  
784  $\mu$ g of inactivated NDV-HXP-S or WT NDV (negative control). Two immunizations were performed via  
785 the intramuscular route at D0 and D21. At D44, mice were treated with Ad5-hACE2. At D49, one third of  
786 mice from each group was challenged with USA-WA1/2020, B.1.351 or P.1 strain. At day 2, lungs were  
787 harvested and homogenized in 1 mL PBS. Viral titers were measured by plaque assay on Vero E6 cells  
788 and plotted as GMT of PFU/mL (LoD=50 PFU/mL; A titer of 25 PFU/mL was assigned to negative  
789 samples). Statistical difference was analyzed by one-tailed t test. The p values are indicated.

790  
791 **Figure S1. Vaccination with inactivated and live NDV-HXP-S favors a IgG2a production over**  
792 **IgG1.** ELISAs were performed using either anti-mouse IgG2a or IgG1 secondary antibody to determine  
793 subclasses of IgG induced by (A) inactivated NDV-HXP-S related to the mouse study described in Figure  
794 2 or (B) live NDV-HXP-S related to the mouse study described in Figure 6. GMT AUC was plotted.

795  
796 **Figure S2. Inactivated NDV-HXP-S reduces SARS-CoV-2 induced lung pathology in hamsters.**  
797 Related to the hamster study in Figure 4, Left lung lobes of hamsters collected at day 5 post-challenge

798 were fixed in neutral buffered formalin and cut into 5µm sections and stained with hematoxylin and eosin  
799 (H&E). All sections were evaluated by a veterinary pathologist who was blinded to the vaccination  
800 groups to score (A) Amount of lung affected; (B) Perivascular inflammation; (C) Alveolar inflammation  
801 and necrosis/fibrin; (D) Type II pneumocytes hyperplasia/cytopathy and (E) Epithelial  
802 degeneration/necrosis, bronchial/bronchiolar inflammation, intraluminal debris.

803

804 **Figure S3. Live NDV-HXP-S induces spike-specific mucosal IgA.** Nasal washes were collected from  
805 mice that were vaccinated with 10<sup>6</sup> EID<sub>50</sub> of NDV-HXP-S or WT NDV (negative control) intranasally 3  
806 weeks later. Spike-specific IgA in the nasal washes was measured by ELISAs.

807

808

809

810

811

# Figures

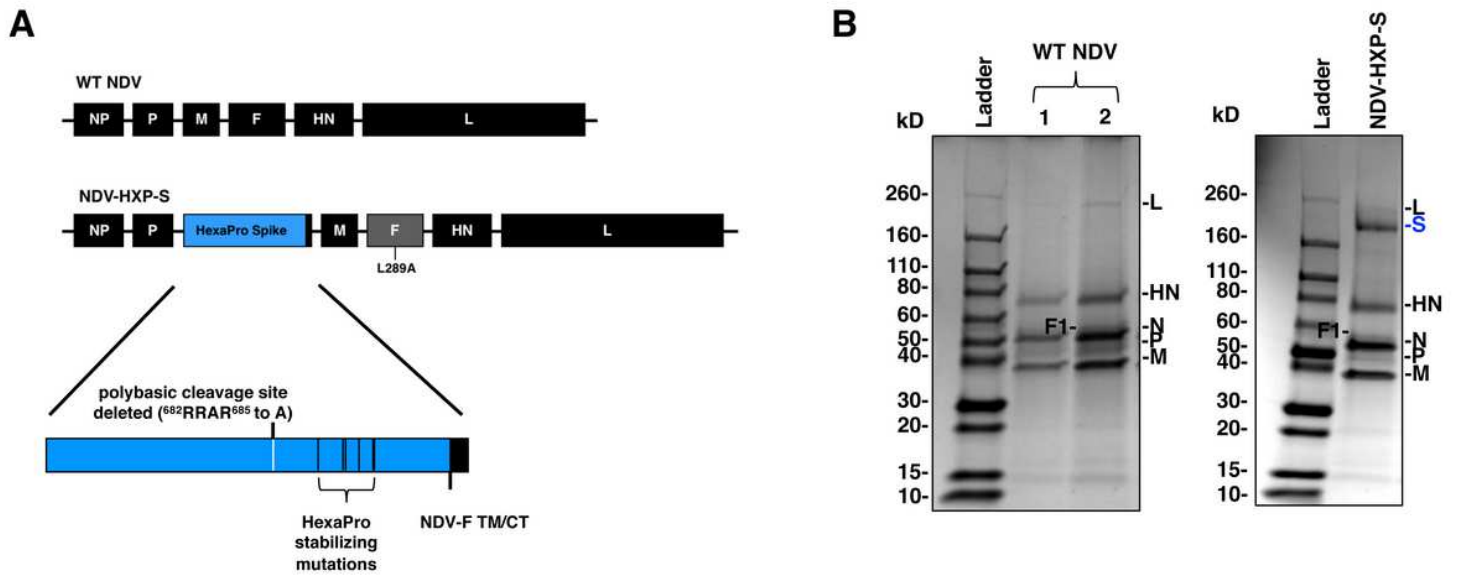


Figure 1

Figure 1

Design of the NDV-HXP-S construct.

Figure 2

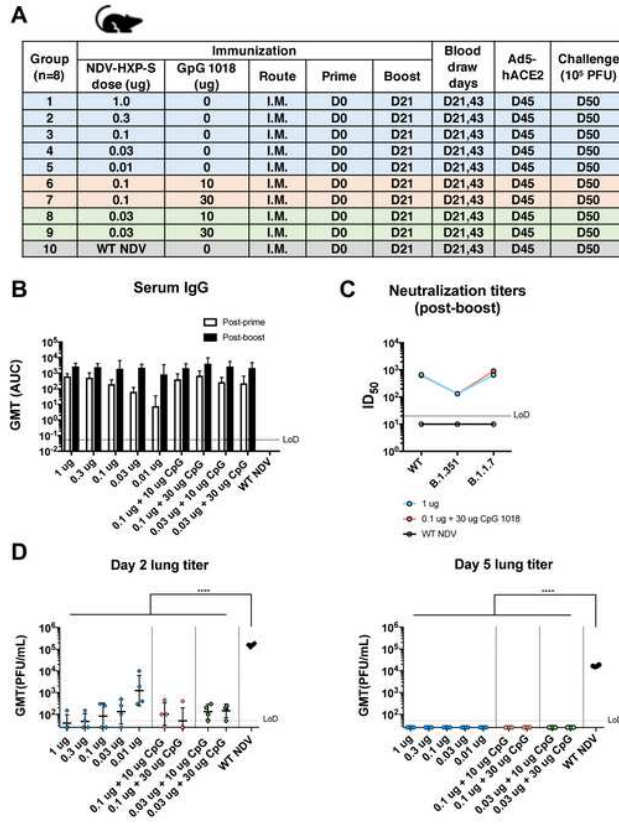


Figure 2

Low doses of inactivated NDV-HXP-S induce protective antibody response in mice.

Figure 3

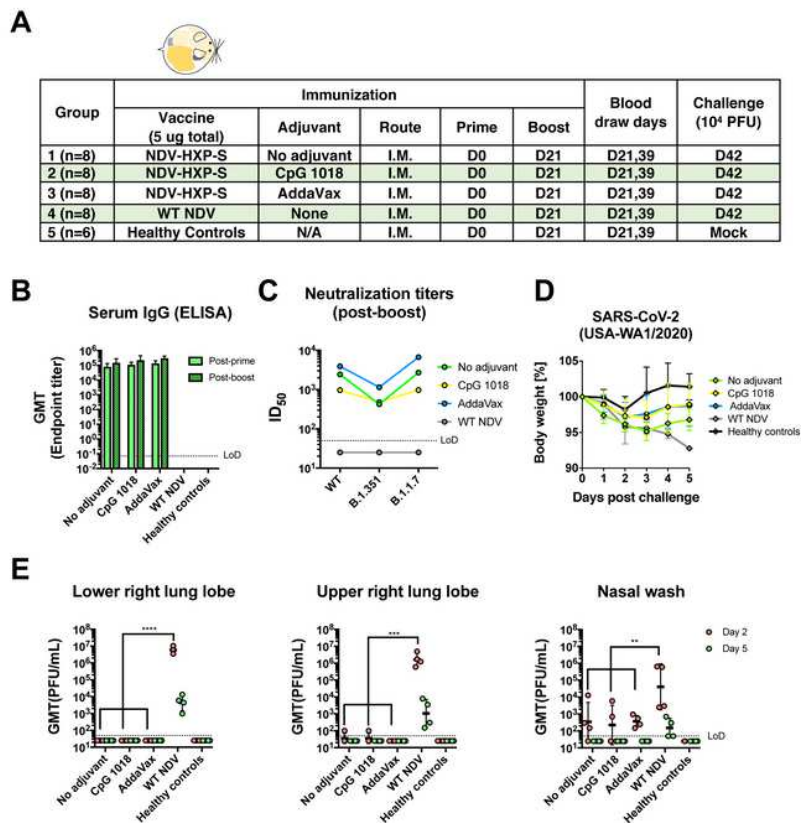
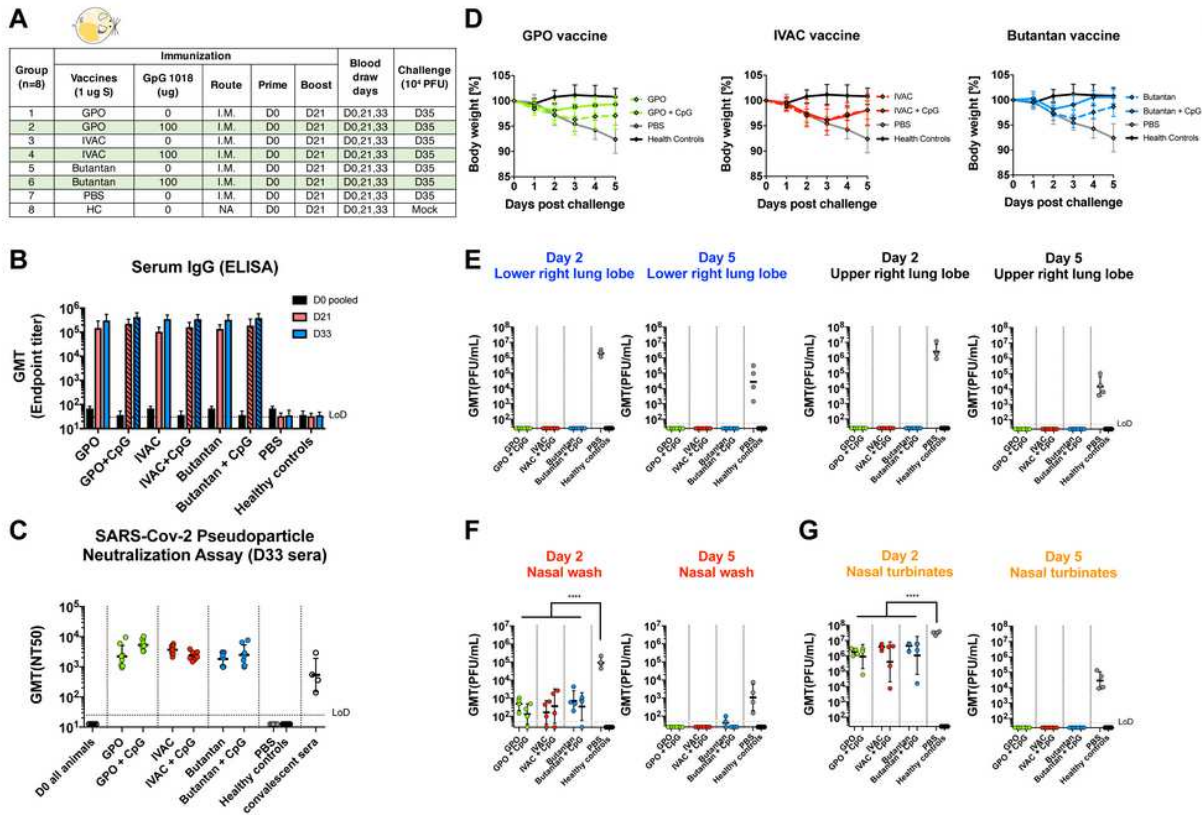


Figure 3

**Figure 3**

Inactivated NDV-HXP-S induces protective antibody response in hamsters.



**Figure 4**

**Figure 4**

GMP lots of inactivated NDV-HXP-S produced by influenza virus vaccine manufacturers induce protective antibody response in hamsters.

Figure 5

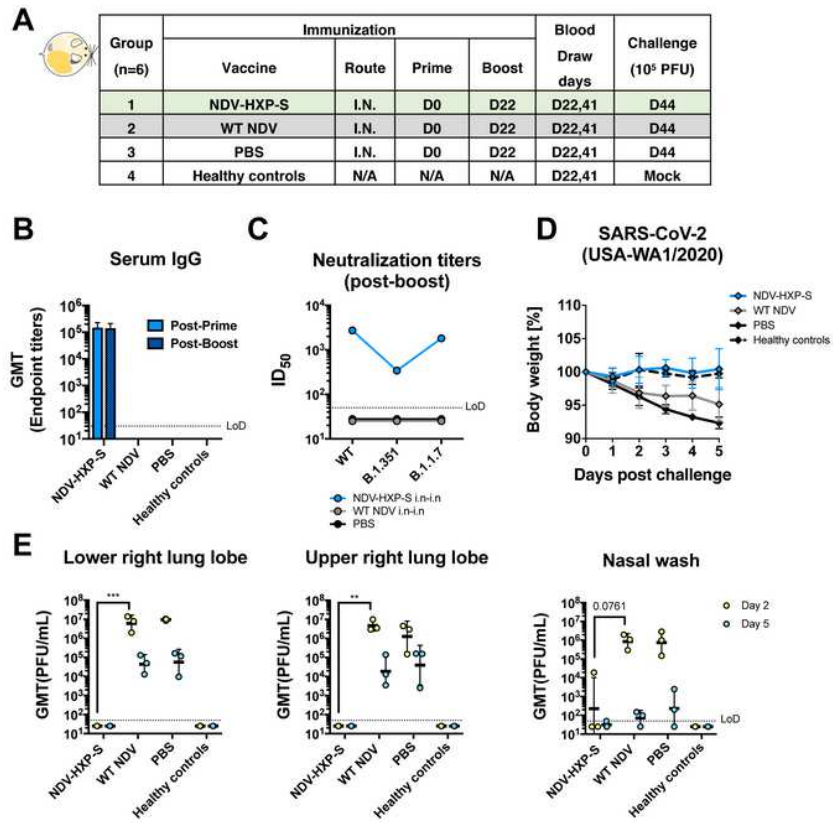


Figure 5

Live NDV-HXP-S via the intranasal route induces protective antibody responses in hamsters.

Figure 6

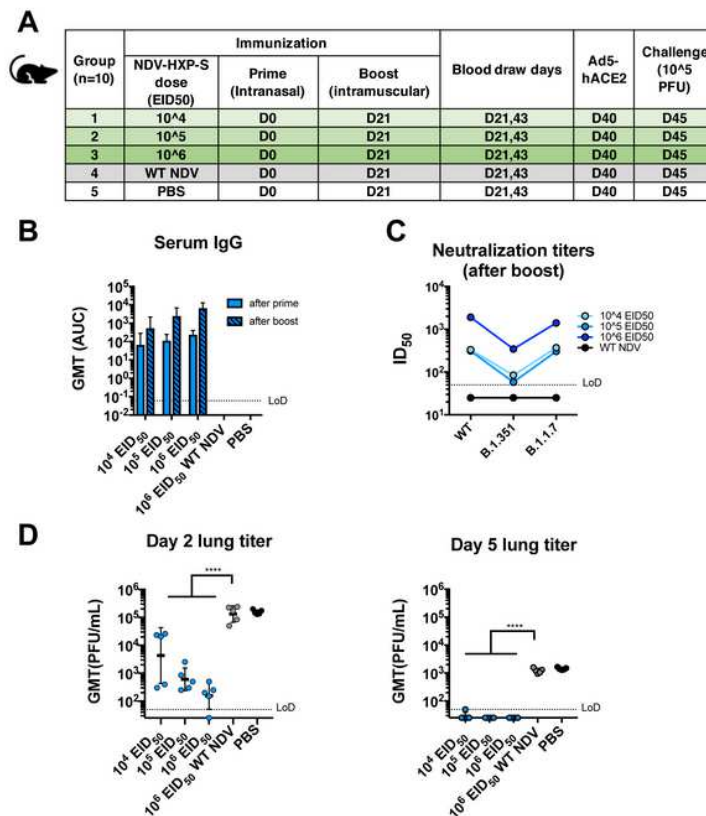
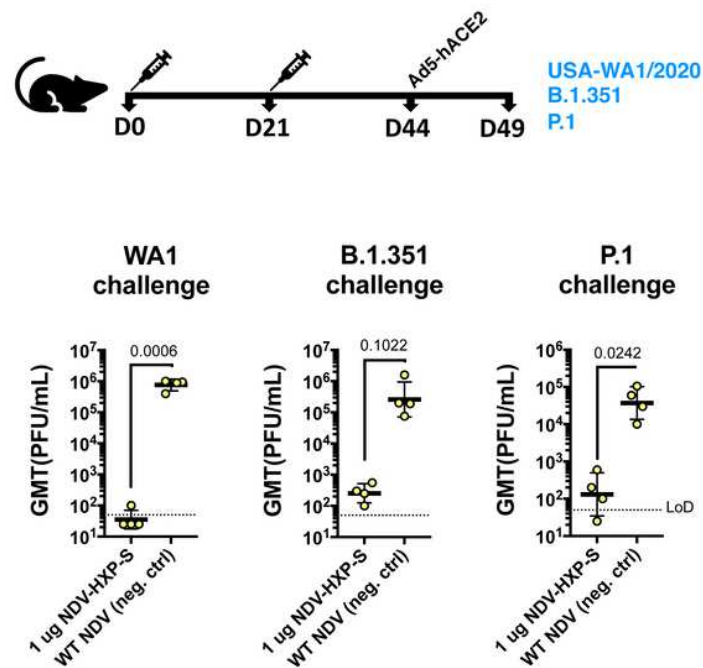


Figure 6

**Figure 6**

Intranasal prime followed by intramuscular boost of live NDV-HXP-S induces protective antibody responses in mice.



**Figure 7**

**Figure 7**

Inactivated NDV-HXP-S induces protective antibody response against challenge of SARS-CoV-2 variants of concern.

## Supplementary Files

This is a list of supplementary files associated with this preprint. Click to download.

- [SupplementaryFigure1.png](#)
- [SupplementaryFigure2.png](#)
- [SupplementaryFigure3.png](#)